Research Article | Vol. 10, No. 2 / 1 February 2020 / Optical Materials Express 674
Optical Materials EXPRESS

Femtosecond laser-induced periodic surface structures formation on bismuth thin films upon irradiation in ambient air

RICARDO SANTILLAN,[1] ABRAHAM WONG,[1] PAULINA SEGOVIA,[2,4] MARCO CAMACHO-LOPEZ,[3] AND SANTIAGO CAMACHO-LOPEZ[1,5]

[1]*Optics Department, Centro de Investigacion Cientifica y de Educacion Superior de Ensenada, Carretera Ensenada-Tijuana No. 3918, Zona Playitas, Ensenada, Baja California, 22860, Mexico*
[2]*Catedras CONACYT, Centro de Investigacion Cientifica y de Educacion Superior de Ensenada, Carretera Ensenada-Tijuana, No. 3918, Zona Playitas, 22860, Ensenada, Baja California, Mexico*
[3]*Laboratorio de Investigacion y Desarrollo de Materiales Avanzados, Facultad de Quimica, Universidad Autonoma del Estado de Mexico, Campus Rosedal, Km 14.5 Carretera Toluca-Atlacomulco, San Cayetano de Morelos, Toluca, C.P. 50295, Mexico*
[4]*psegovia@cicese.mx*
[5]*camachol@cicese.mx*

Abstract: The formation of laser-induced periodic surface structures (LIPSS) on a bismuth thin film with a femtosecond laser is reported for the first time. The surface structures were generated at normal incidence in air environment with fluence below the ablation threshold. The effect of the number of pulses on the LIPSS morphology and on their chemical composition was investigated. The results show the generation of low spatial frequency LIPSS (LSFL), accompanied by regularly distributed nanoparticles. The LIPSS are oriented perpendicular to the laser polarization with a period ΛLSFL that doesn't show a significant variation with the number of pulses (~1μm). In contrast to previous studies for LIPSS formation on bismuth films under ns laser irradiation [Opt. Mater. Express, **7**(6), 1777-1786 (2017)], in the present case no oxidation was observed.

1. Introduction

Laser-induced periodic surface structures (LIPSS) are a universal phenomenon that can be generated on almost any material upon linearly polarized radiation. These structures can be produced with continuous or pulsed laser light and their formation process and features are strongly dependent on the type of material and irradiation parameters [1]. Depending on their periodicity, LIPSS can be classified in two types: low spatial frequency LIPSS (LSFL) with periods approximately equal to the wavelength of the incident field and high spatial frequency LIPSS (HSFL) with periods significantly smaller than the irradiation wavelength, in the order of half the wavelength or even shorter. For metals the orientation of LSFL is generally perpendicular to the polarization of the irradiation beam, while for HSFL it can be either parallel or orthogonal [1]. In this context, one of the most accepted theories to explain LSFL formation is described as an interference of the incident laser beam with a surface electromagnetic wave (SEW) generated at the rough surface, which might include the excitation of surface plasmon polaritons (SPPs) [2]. Furthermore, the physical mechanism to explain the formation of HSFL is still controversially discussed in the literature [1]. Particularly for structures induced by femtosecond (fs) laser pulses, the LSFL period also seems to present a dependency on both the number of pulses and fluence [3]. From the technological point of view, LIPSS have attracted remarkable interest due its one-step process; and it has been proven that in air environment it provides a reliable nanostructuring technique [4]. These structures offer the opportunity of controlling the optical, chemical, electrical and mechanical properties of surfaces. For this reason, LIPSS

#384019 https://doi.org/10.1364/OME.384019
Journal © 2020 Received 25 Nov 2019; revised 16 Dec 2019; accepted 17 Dec 2019; published 30 Jan 2020

Optical Materials EXPRESS

have been proposed to be used in photonics, plasmonics, or even industrial applications such as micromachining, color marking, micro fluidic technologies and micro electromechanical systems [5–7]. Bismuth (Bi) is a very interesting material not only due to its thermal and electrical attributes, but also because of the optical properties of its nanostructured form [8,9]. In addition, Bi is found to be a versatile material in thin film laser processing [9,10]. LIPSS formation on the surface of Bi can significantly change the physical properties of this material, leading to some new applications. Bi_2O_3 has been generated in Bi with continuous wave (CW) or pulsed laser irradiation [10–14]. Also, the formation of LIPSS in Bi thin films by nanosecond pulsed laser irradiation was demonstrated in some prevoius work [8,9]. In that case, LIPSS created on the surface of the Bi film exhibited an orientation perpendicular to the laser polarization with periodicity on the order of the irradiation wavelength. Although the laser irradiation for a low number of pulses (20-50) was performed in air the formed LIPSS are oxidation free, in fact when bismuth oxide forms for a large number of pulses (600) LIPSS vanish [8]. In this article, we present an experimental study where it is reported, for first time to the best of our knowledge, the formation of oxide-free Bi LIPSS, below the ablation threshold, under femtosecond pulsed laser irradiation in ambient air.

2. Material and methods

2.1. fs-laser irradiation

Bismuth thin films, with 400 nm thickness, were fabricated by the Ar ion DC-sputtering technique and the films were grown onto glass substrates. The average roughness of the film obtained by Atomic Force Microscopy (AFM) measurements is 34 nm. The irradiations were performed with the experimental setup shown in Fig. 1. A commercial Ytterbium-doped fiber laser amplifier system (Satsuma Amplitude HP2) was used to generate linearly polarized 270 fs laser pulses, at a central wavelength of $\lambda = 1030$ nm, and it was operated at a pulse repetition rate of 10 kHz. Through the phenomenological model described in [15], the laser ablation threshold for the sample was determined to be 62 mJ/cm^2 per pulse with an incubation coefficient of 0.9. Considering the low melting point of bismuth (271°C) the irradiations were carried out at a per

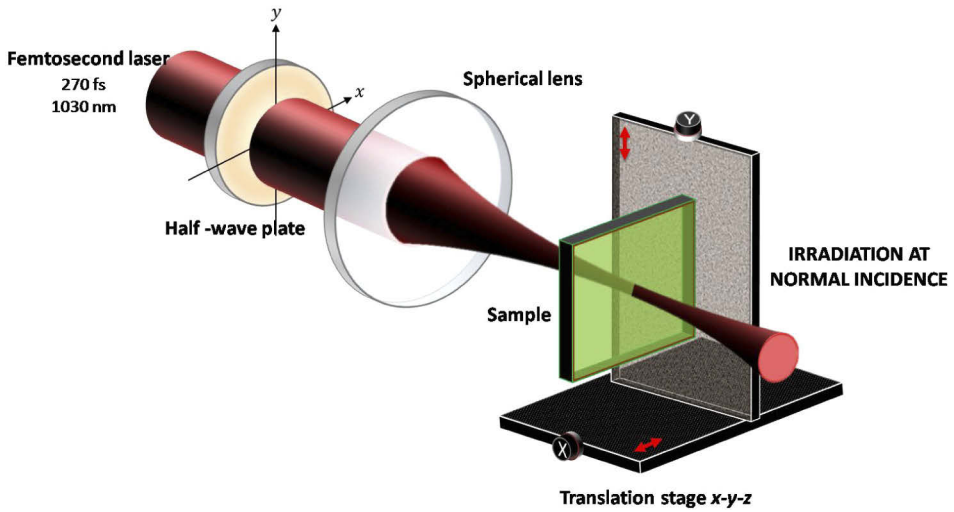

Fig. 1. Experimental setup. The fs-pulse (270 fs, 10 kHz, $\lambda = 1030$ nm) laser beam is focused through a spherical lens (f = 150 mm) on the sample. The translation stage controls the sample displacement along the x, y or z. All irradiations were performed in ambient air.

Optical Materials EXPRESS

pulse laser fluence of 16.8mJ/cm^2, where the material removal mechanisms such as spalling do not occur. The laser beam was focused on the sample by a spherical lens with f = 150 mm focal length. The obtained beam waist diameter was $2\omega_0 = 90$ µm (FW1/e^2). The polarization of the incoming radiation was controlled by rotation of a half-wave plate on a rotary stage. The bismuth film sample was conveniently mounted on a motorized xyz linear translation stage (Sigma Koki Co. SG-SP20-85) for controlled displacement during the irradiations. Multi-pulse experiments were performed using a digital delay/pulse generator (SRS DG645) synchronized to the laser to gate the number of pulses (N) delivered to the film.

2.2. LIPSS characterization

After the irradiations, the chemical composition on the sample surface was examined by microRaman spectroscopy (HR-800 LabRaman, Jobin-Yvon-Horiba). The Raman spectra measurements were performed with a CW He-Ne laser $\lambda = 632.8$ nm with 75 µW laser power on the sample. All Raman spectra were collected by using a diffraction grating of 1800 l/mm, in the 50-365 cm^{-1} range. These spectra were obtained using an average of 10 acquisitions with an integration time of 60 seconds per frame. The irradiated regions were also analyzed with Optical Microscopy - OM (BX41, Olympus), Scanning Electron Microscopy - SEM (Hitachi SU3500) and Atomic Force Microscopy- AFM (NanoSurf Flex-Axiom).

3. Results and discussion

3.1. LIPSS characterized by OM, SEM, and AFM

An analysis of the LIPSS formation in Bi was performed for a fixed per pulse fluence F = 16.8 mJ/cm^2 with a repetition rate f = 10 kHz. Figure 2 shows optical micrographs of the surface of both the non-irradiated Bi film and after being irradiated with 100 and 200 laser pulses.

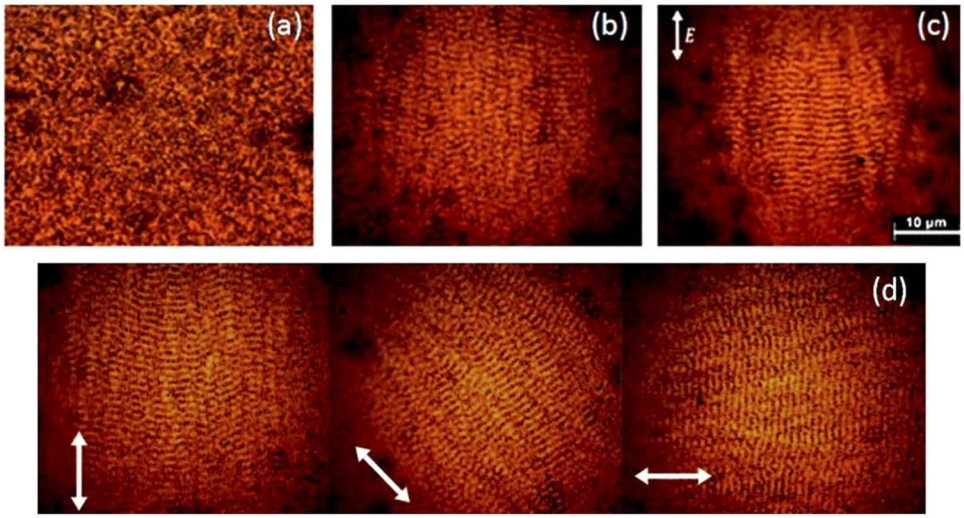

Fig. 2. Optical micrographs showing the surface morphology of the non-irradiated bismuth film (a) and the structures formed with N = 100 (b), N = 200 (c). LIPSS orientation as a function of the pulses polarization direction at 0°, 45° and 90° (d).

It can be clearly observed how the initially granular Bi surface turns into the incipient formation of LIPSS for N = 100 (Fig. 2(b)), while a two fold increase of N results in the formation of well-defined LIPSS structures with orientation perpendicular to the laser light polarization (Fig. 2(c)). As expected the LIPSS orientation shows a strong dependence on the polarization

Optical Materials EXPRESS

of the incident laser light as it can be seen in Fig. 2(d). To further investigate in detail on the formation process of LIPSS by multiple pulses on a single spot and a fixed per pulse fluence, irradiations with N = 50, 100, 150 and 200 were carried on. Figure 3(b-e) shows SEM images of the LIPSS formed at the surface of the thin film. With an increasing number of pulses, the LIPSS structure becomes better defined; this is evidenced by the appearance of two bright spots in the 2D Fourier patterns shown in the insets of Fig. 3(c-e).

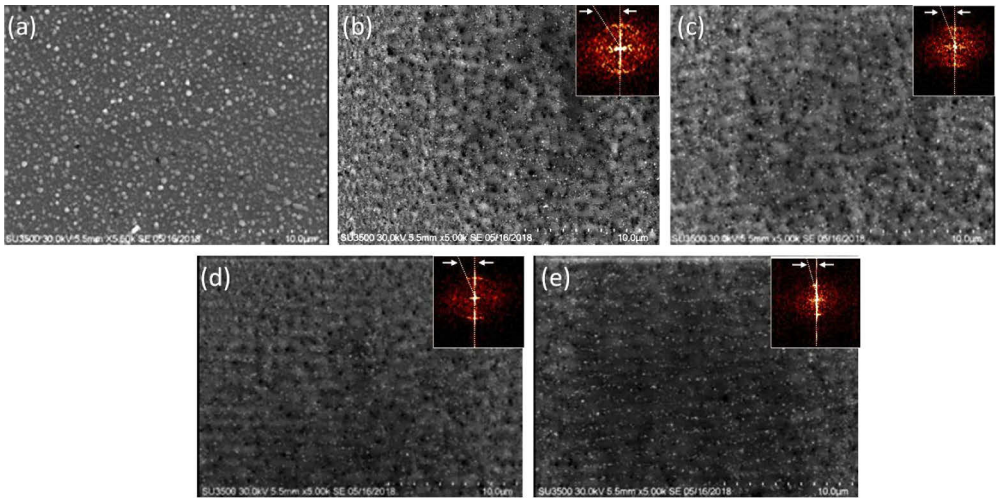

Fig. 3. SEM micrographs of the thin film prior to be irradiated (a), LIPSS formation induced at different number of pulses (b) 50, at different number of pulses (c) 100, (d) 150, (e) 200 and their corresponding FFT (inset).

The spatial period of the Bi LIPSS as a function of the number of pulses was estimated using the 2D Fourier patterns from the SEM images (Fig. 3). The results of the analysis (Fig. 4) shows that even do the periodicity seems to vary with the number of pulses (from 1040 down to 980 nm), the error bars make this variation of low significance. Such a periodicity, and the LIPSS perpendicular orientation to the incident laser beam polarization, demonstrates the formation of LSFL whose origin in metals (in this case the semi-metal Bi) is generally attributed to the interference of the incident laser beam with SPPs [2].

The morphological characteristics of the LIPSS can be studied in more detail through AFM measurements. Figure 5 shows the AFM images for LIPSS formed at N = 50, 100, 150 and 200.

A regular distribution of nanoparticles, which follows the LIPSS orientation, can be observed across the structured surface. These nanoparticles can be seen as tiny bright spots in both AFM and SEM images. The low melting point of Bi may give place to nanoparticle nucleation from evaporated and redeposited material. A similar effect of regular nanostructures forming on top and along LIPSS was observed in [4], where nanocraters were nucleated on TiO_2 LIPSS produced by nanosecond laser pulses on Ti thin films. It is interesting to notice that in the present work with the increase of N, there is a significant redistribution of nanoparticles and those are concentrated mainly on the regions with lower energy. This dissemination is attributed to the interference maximum of the energy distribution, where the energy density becomes enough for vaporization of the material [16]. It is also important to point out that this nanoparticle redistribution contributes to the regularity of the LIPSS. On the nucleated nanoparticles, it is not clear from the SEM micrographs if the size of the nanoparticles changes with N at all. However, by analyzing the grain size distribution in the AFM images, using Gwyddion and selecting the mean value, we noticed that the overall grain size varies such that the largest grain size (195 nm) is obtained for N = 150, while the smallest grain size (143 nm) was obtained for N = 200.

Optical Materials EXPRESS

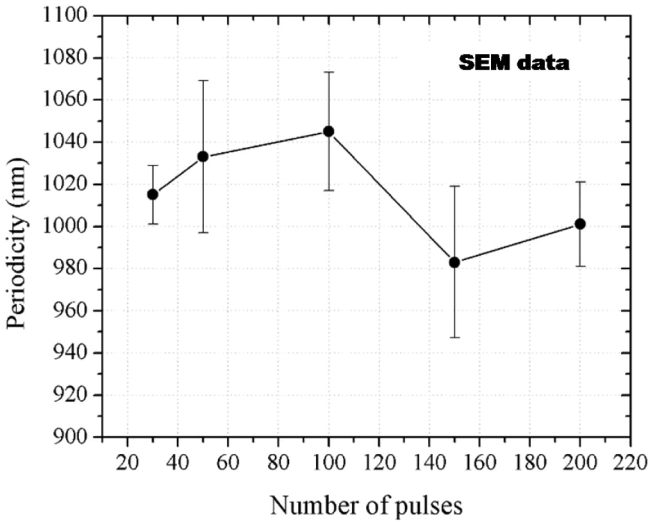

Fig. 4. Spatial periods of the LSFL for different number of pulses obtained from their corresponding FFT.

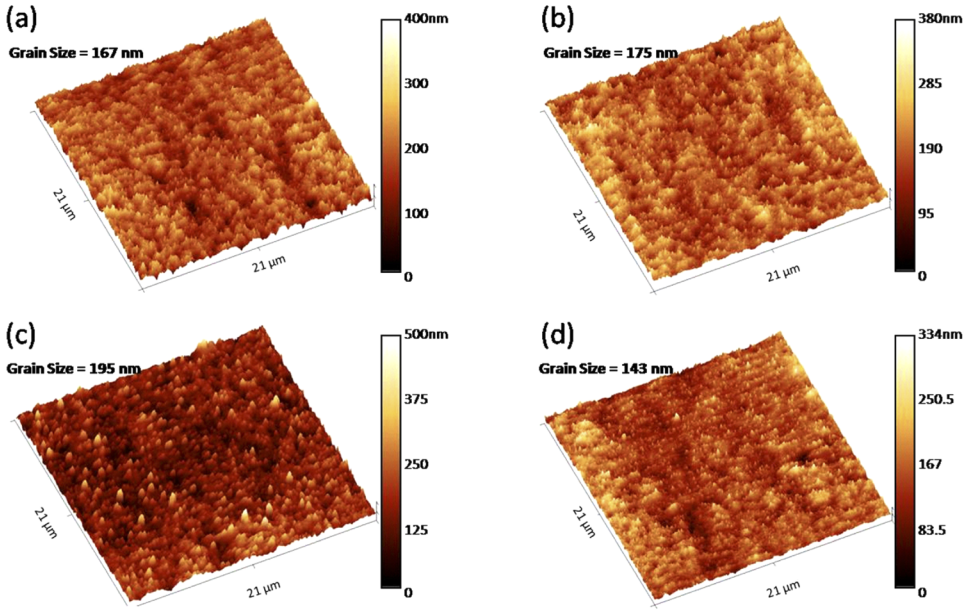

Fig. 5. AFM topography images ($21 \times 21 \mu m^2$) of Bi irradiated with (a) 50, (b) 100, (c) 150 and (d) 200 pulses. The mean value of the grain size of each structure is indicated for every single image.

Optical Materials EXPRESS

3.2. LIPSS composition

Examining the Raman spectra of the as-deposited and the laser irradiated bismuth film for N = 50, 100, 150 and 200 (Fig. 6) it was possible to determine the chemical composition of the LIPSS.

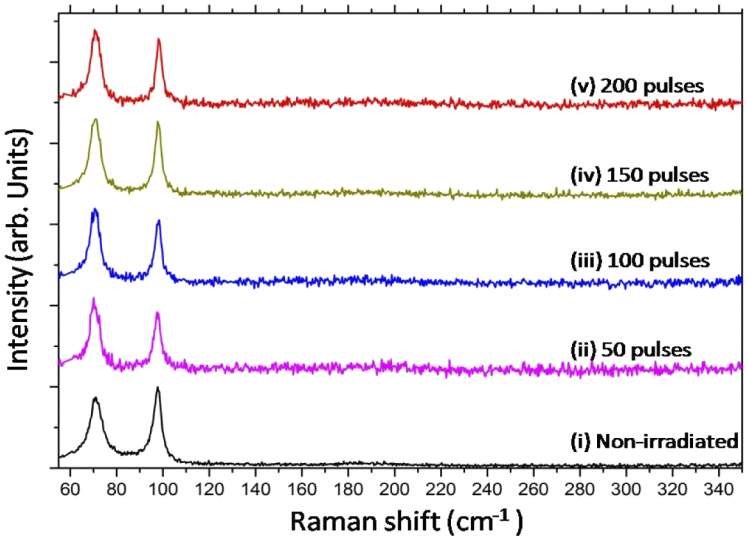

Fig. 6. Raman spectra for the non-irradiated bismuth film(i), irradiated spot with 50 (ii), 100 (iii), 150 (iv) and 200 (v) pulses.

These spectra remain the same for both the non-irradiated and the irradiated analyzed spots on the sample. All the spectra show two characteristic peaks at 70 and 98 cm^{-1}, which correspond to the Raman bands, assigned to the Bi-Bi vibrations and the lattice vibration, respectively [10–13]. The change in the relative intensity between the bands indicates that the Bi LIPSS went through a change on its crystallographic orientation. Noticeable, N does not affect the chemical composition of the surface; although the laser irradiation is carried out in air no signs of laser-induced oxidation appeared at all. This result shows novelty if compared to [8], where it was shown that for a large number (hundreds) of nanosecond laser pulses, and processing in air, Bi LIPSS vanish to give rise the formation of Bi_2O_3 agglomerates. In the present case, under these circumstances it could also be expected that bare Bi constitutes the nucleated nanoparticles observed in the SEM and AFM micrographs.

3.3. LIPSS formation

This interference mechanism [2] predicts a LIPSS periodicity (Λ_{LIPSS}) smaller than the incident wavelength λ, which is given by [17]:

$$\Lambda_{LIPSS} = \frac{\lambda}{\frac{\lambda}{\lambda_{SPP}} \pm \sin\theta}, \tag{1}$$

where θ is the angle of incidence and λ_{SPP} stands for the SPP wavelength [18] :

$$\lambda_{SPP} = \lambda \mathrm{Re}\left[\frac{\varepsilon + \varepsilon_d}{\varepsilon\varepsilon_d}\right]^{1/2} \tag{2}$$

The bismuth LSFL exhibits these features, i.e. a period close to the irradiation wavelength and an orientation perpendicular to the laser beam polarization (Fig. 2). For the particular case of

Optical Materials EXPRESS

normal incidence irradiation on the interface air-bismuth ($\varepsilon = -3.5332 + 34.259i$ at $\lambda = 1.03$ μm [19], $\varepsilon_d \approx 1$) the predicted periodicity, according to Eq.1, reduces to $\Lambda_{LIPSS} = \lambda_{SPP}$, i.e. $\Lambda_{LIPSS} \approx$ 1028 nm, which is in very good agreement with the experimental results for N = 50. In order to study the impact of N on the LIPSS morphology, their regularity was investigated. The structures were analyzed by measuring the dispersion of the LIPSS orientation angle, DLOA, from SEM images (Fig. 7).

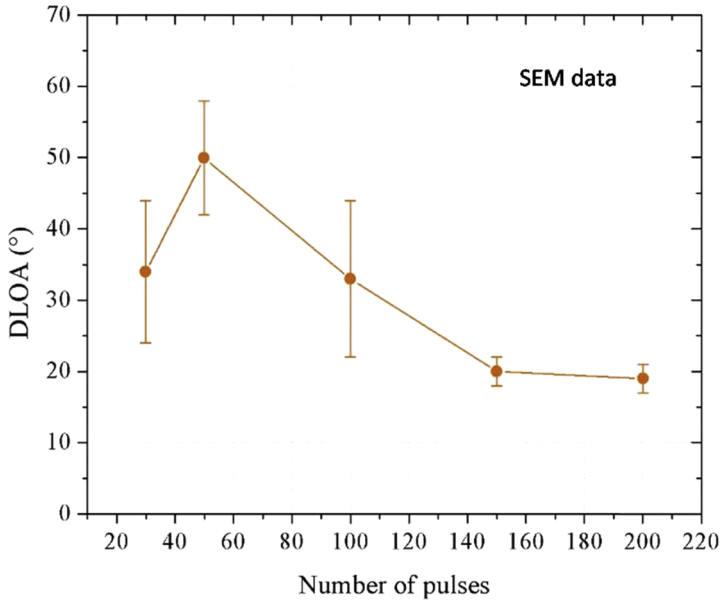

Fig. 7. Effect of the number of pulses on the DLOA obtained from the FTT images of the SEM micrographs.

At N = 50 the LIPSS exhibit the lowest regularity with a DLOA of 50 °. For N ≥ 150 the LIPSS become better defined on the surface of the sample, and its regularity significantly improves producing a DLOA of 18° for N = 200.

4. Conclusions

Low spatial frequency LIPSS have been demonstrated on Bi thin films by using fs-laser pulses with fluence below the ablation threshold. The LSFL follow the periodicity and orientation predicted by the model that considers the interference of the incident field with the SPPs excited in the Bi surface. Usually, shorter periods are obtained for increasing number of pulses, this behavior is a consequence of inter and intra-pulse feedback mechanisms and has been observed in different materials [12]. However, in this case, the experimental results show that LIPSS period is not significantly affected by N. A possible explanation for this behavior is that, according with the incubation coefficient for the used pulse repetition rate, the contribution by incubation effects is very low. Remarkably, regularly ordered nanoparticles nucleated on top of the LSFL following the LIPSS orientation. The nanoparticles formation could be a result of the re-deposition of evaporated Bi constituting a feedback process. The increasing roughness on the film, originated by the first pulses, facilitates the coupling of energy on the surface producing hot spots, where, the localized field favors the evaporation process. On the evolution of the LIPSS formation, the regularity of the LIPSS improves with the number of pulses N, this is assessed by the DLOA (Dispersion of the LIPSS Orientation Angle). In comparison with [8], and no matter the laser processing is carried out in ambient air a chemical modification of the surface, even for hundreds

Optical Materials EXPRESS

of pulses, does not take place. This is a consequence of the ultrashort nature, and relative low repetition rate of the laser pulses that prevents thermal cumulative effects as the ones observed when using long ns laser pulses.

Funding

Consejo Nacional de Ciencia y Tecnología (CB17-18-A1-S-21245, CB-2015-01-254304, FONCICyT- 246648).

Acknowledgement

Authors thank the program Catedras-CONACYT. Also, authors acknowledge M Eng. Fabián Alonso-Cordero and Dr. Marcos Plata-Sanchez and MSc Alejandro Esparza for their technical support with the SEM and AFM and fabrication of the samples, respectively.

References

1. J. Bonse, S. Höhm, S. V. Kirner, A. Rosenfeld, and J. Krüger, "Laser-induced periodic surface Structures, a scientific evergreen," IEEE J. Sel. Top. Quantum Electron. **23**(3), 9000615 (2017).
2. J. Bonse, A. Rosenfeld, and J. Krüger, "On the role of surface plasmon polaritons in the formation of laser-induced periodic surface structures upon irradiation of silicon by femtosecond-laser pulses," J. Appl. Phys. **106**(10), 104910 (2009).
3. K. Okamuro, M. Hashida, Y. Miyasaka, Y. Ikuta, S. Tokita, and S. Sakabe, "Laser fluence dependence of periodic grating structures formed on metal surfaces under femtosecond laser pulse irradiation," Phys. Rev. B **82**(16), 165417 (2010).
4. S. Camacho López, R. Evans, L. Escobar Alarcón, M. A. Camacho López, and M. A. Camacho López, "Polarization-dependent single-beam laser-induced grating-like effects on Titanium films," Appl. Surf. Sci. **255**(5), 3028–3032 (2008).
5. A. Y. Vorobyev and C. Guo, "Colorizing Metals with Femtosecond Laser Pulses," Opt. Photonics News **19**(12), 30 (2008).
6. L. Guoqiang, L. Jiawen, H. Yanlei, Z. Chenchu, L. Xiaohong, C. Jiaru, and H. Wenhao, "Femtosecond laser color marking stainless steel surface with different wavelengths," Appl. Phys. A **118**(4), 1189–1196 (2015).
7. B. Dusser, Z. Sagan, H. Soder, N. Faure, J. P. Colombier, M. Jourlin, and E. Audouard, "Controlled nanostructures formation by ultra-fastlaser pulses for color marking," Opt. Express **18**(3), 2913–2924 (2010).
8. A. Reyes-Contreras, M. Camacho-Lopez, S. Camacho-Lopez, O. Olea-Mejia, A. Esparza-García, J. G. Bañuelos-Muñeton, and M. A. Camacho-Lopez, "Laser-induced periodic surface structures on bismuth thin films with ns laser pulses below ablation threshold," Opt. Mater. Express **7**(6), 1777–1786 (2017).
9. A. Reyes-Contreras, M. A. Camacho-Lopez, E. Camps, and L. E. Romero-Salazar, "Study of LIPSS formation on bismuth thin films deposited by pulsed laser deposition," Superficies y Vacío. **31**, 39–42 (2018).
10. L. Kumari, J.-H. Lin, and Y.-R. Ma, "Laser oxidation and wide-band photoluminescence of thermal evaporated bismuth thin films," J. Phys. D: Appl. Phys. **41**(2), 025405 (2008).
11. M. A. Zepeda, M. Picquart, and E. Haro-Poniatowski, "Laser induced oxidation effects in bismuth thin films," Mater. Res. Soc. Symp. Proc. **1477**, imrc12-1477-s1a-p016 (2012).
12. J. A. Steele and R. A. Lewis, "In situ micro-Raman studies of laser-induced bismuth oxidation reveals metastability of β-Bi_2O_3microislands," Opt. Mater. Express **4**(10), 2133–2142 (2014).
13. C. Díaz-Guerra, P. Almodóvar, M. Camacho-Lopez, S. Camacho-López, and J. Piqueras, "Formation of β-Bi_2O_3 and δ-Bi_2O_3 during laser irradiation of Bi films studied in-situ by spatially resolved Raman spectroscopy," J. Alloys Compd. **723**, 520–526 (2017).
14. A. Venegas-Castro, A. Reyes-Contreras, M. Camacho-López, O. Olea-Mejía, S. Camacho-López, and A. Esparza-García, "Study of the integrated fluence threshold condition for the formation of β-Bi_2O_3 on Bi thin films by using ns laser pulses," Opt. Laser Technol. **81**, 50–54 (2016).
15. Y. Jee, M. F. Becker, and R. M. Walser, "Laser-induced damage on single-crystal metal surfaces," J. Opt. Soc. Am. B **5**(3), 648–659 (1988).
16. A. Y. Vorobyev and C. Guo, "Effects of nanostructure covered femtosecond laser-induced periodic surface structures on optical absorptance of metals," Appl. Phys. A **86**(3), 321–324 (2007).
17. F. Keilmann and Y. H. Bai, "Periodic surface structures frozen into CO_2 laser-melted quartz," Appl. Phys. A **29**(1), 9–18 (1982).
18. H. Raether, *Surface Plasmons on Smooth and Rough Surfaces and on Gratings* (Springer-Verlag, 1988).
19. H. J. Hagemann, W. Gudat, and C. Kunz, "Optical constants from the far infrared to the x-ray region: Mg, Al, Cu, Ag, Au, Bi, C, and Al_2O_3," J. Opt. Soc. Am. **65**(6), 742–744 (1975).